Available online at www.sciencedirect.com
SCIENCE DIRECT®
Journal of Solid State Chemistry 177 (2004) 3610–3615
JOURNAL OF SOLID STATE CHEMISTRY
http://elsevier.com/locate/jssc

On the characterization of $BiMO_2NO_3$ (M = Pb, Ca, Sr, Ba) materials related with the Sillén X_1 structure

Peter Ziegler,[a] Inga Grigoraviciute,[b] Katharina Gibson,[a] Jochen Glaser,[a] Aivaras Kareiva,[b] and H.-Jürgen Meyer[a,*]

[a] *Abteilung für Festkörperchemie und Theoretische Anorganische Chemie, Eberhard-Karls-Universität, Auf der Morgenstelle 18, Tübingen D-72076, Germany*

[b] *Department of General and Inorganic Chemistry, Vilnius University, Naugarduko 24, Vilnius LT-2006, Lithuania*

Received 11 December 2003; received in revised form 16 March 2004; accepted 21 March 2004

Abstract

The compounds $BiMO_2NO_3$, with M= Pb, Ca, Sr, and Ba, were obtained as single-phase products from solid-state reactions in an atmosphere of nitrous gases. The oxide nitrates with Pb and Ca crystallize in the tetragonal space group *I*4/*mmm* with two formula units per unit cell; the oxide nitrates with Sr and Ba crystallize in the orthorhombic space group *Cmmm* with four formula units per unit cell. Lattice parameters at room temperature are $a = 397.199(4)$, $c = 1482.57(2)$ pm for M= Pb; $a = 396.337(5)$, $c = 1412.83(3)$ pm for M= Ca; $a = 1448.76(3)$, $b = 567.62(1)$, $c = 582.40(1)$ pm for M= Sr and $a = 1536.50(8)$, $b = 571.67(3)$, $c = 597.55(3)$ pm for M= Ba. The structures, which were refined by powder X-ray diffraction, consist of alternating $[BiMO_2]^+$ and $[NO_3]^-$ layers stacked along the direction of the long axis. IR and thermogravimetric data are also given. The various M^{2+} cations in $BiMO_2NO_3$ are compatible with each other; therefore and because of their layer-type structure, these compounds are interesting precursors for oxide materials, e.g., the HTSC compounds $(Bi,Pb)_2Sr_2Ca_{n-1}Cu_nO_x$.

Keywords: Bismuth; Oxide nitrates; Crystal structures; Cation ordering; Sillén phases

1. Introduction

A structure series of oxide halides originally investigated by Sillén [1,2] consists of fluorite related cationic $[M_2O_2]$ layers (M= Bi, Sb, Pb, Cd, Ca, Sr, Ba, Li, Na) separated by halide layers. Sillén adopted the notation X_n (n = 1, 2, 3) to indicate the number of halide layers separating the metal oxide layers. Two examples of these phases are $BiPbO_2I$ [3] (X_1 type) and BiOI [4] (X_2 type). Combinations of these structures are found in, e.g., $Bi_3SrO_4Br_3$ (X_1X_2) and $Bi_2SrO_3Br_2$ ($X_1X_1X_2$) [5]. The oxide layers in both structures can be replaced by fluoride, for the X_1 type in $APbF_2X$ (A= Li, Na, K; X= Cl, Br, I) [6] and for the X_2 type in $PbFX$ (X= Cl, Br) [7]. The differences in the ionic radii of the anions prevent mixing of X^- into the close-packed oxide respective fluoride layers, thereby maintaining the layer integrity of the uniquely ordered structures. These layer sequences result in ideal tetragonal structures with $a \sim 390$ pm (i.e., a(fluorite)/$\sqrt{2}$) and c varying from 600 to 5000 pm depending on structural complexity.

The X_1 type bismuth oxide halides $BiMO_2X$ (with X= Cl, Br, I) were initially described as tetragonal (an anti-type to $ThCr_2Si_2$ [8]) with both cations sharing equivalent positions (see Fig. 2a), e.g., $BiPbO_2I$ [3] and $BiCaO_2I$ [9]. This structure type has also been reported for $Bi_2O_2CO_3$ [10], Bi_2O_2Se [11], Nd_2O_2Te [12] and $La_2O_2CN_2$ [13]. However, two different types of cation ordering have been reported for $BiMO_2X$ due to different sizes of the ionic radii of Bi^{3+} and M^{2+}: small M^{2+} like Ca^{2+} [14] give rise to a monoclinic distortion in the oxide chlorides, while the larger Sr^{2+} [9,14] and Ba^{2+} [9,15] generate an orthorhombic superstructure in their respective oxide halides (see Fig. 3c). The latter structure has also been reported for $SbBaO_2Cl$ [16] and $SbPbO_2Cl$ [17–19]. $BiPbO_2Cl$ crystallizes in the orthorhombic structure as the mineral perite [20]; however, synthetic perite has always been reported as tetragonal [3]. The factors which determine the occurrence and type

*Corresponding author. Fax: +49-0-7071295702.
Email-address: juergen.meyer@uni-tuebingen.de (H.-J. Meyer).

0022-4596/$ - see front matter © 2004 Elsevier Inc. All rights reserved.
doi:10.1016/j.jssc.2004.03.027

of cation ordering in quaternary bismuth and antimony X_1 type oxide halides have recently been discussed by Charkin et al. [9].

The compounds we report here also belong to the Sillén X_1 type. Their composition can be derived from the respective $BiMO_2X$ compounds by replacing the halide ion with a nitrate group (NO_3^-). The compositions of the compounds $BiMO_2NO_3$ with M= Pb [21] and Ca [22] have already been described by Kodama, who detected them from thermoanalytical (DTA/TG) studies and mass spectroscopy, and patented their applications as anion-exchange materials. Due to similarities in XRD patterns he expected them to be related with $BiPbO_2I$. In this way he proposed tetragonal cells with the lattice parameters $a = 397.1$ and $c = 1481.9$ pm for M= Pb, and $a = 395.4$ and $c = 1413.1$ pm for M= Ca based on XRD patterns.

2. Experimental procedures and results

Equimolar amounts of $Bi(NO_3)_3 \cdot 5H_2O$ (Fluka, 99%) and $PbCO_3$ (Merck, 99%), $CaCO_3$ (Merck, 99%), $SrCO_3$ (Merck, 99%), or $BaCO_3$ (Merck, 99%) were dissolved in nitric acid (2n) and dried on a magnetic heating stirrer. The residues were carefully ground, filled in a corundum beaker and heated in air (heating rate: 5°C/min; annealing time: 2 h at 350°C for M= Pb, 2 h at 480°C for M= Ca, 2 h at 480°C for M= Sr, 2 h at 360°C for M= Ba). At this point, the solids already contained $BiMO_2NO_3$ as poorly crystalline main phases, but still contained nitrate-rich phases such as $Pb(NO_3)_2$, $Ca(NO_3)_2$, $Sr(NO_3)_2$, or $Ba(NO_3)_2$. In an attempt to purify and crystallize the oxide nitrates and to avoid the formation of oxides, the next reaction step was performed under NO_x atmosphere. The carefully ground mixtures were sealed into evacuated quartz-glass ampoules and heated (heating rate: 5°C/min) to 660°C for M= Pb (annealing time: 160 h), to 690°C for M= Ca (annealing time: 40 h), to 730°C for M= Sr (annealing time: 70 h), and to 730°C for M= Ba (annealing time: 20 h). The reactions yielded yellow powders for M= Pb and Ba and white ones for M= Ca and Sr as well-crystalline single-phase products.

2.1. Structure analyses

Since all attempts to grow crystals to a measurable size were unsuccessful, the crystal structure solutions were accomplished from X-ray powder diffraction data. The employed transmission diffractometer STADI-P (STOE, Darmstadt) used Cu$K\alpha_1$ radiation. The germanium monochromated X-rays have been collected with a linear PSD (opening angle: $2\theta = 6°$). The angular range of the measurements, the step sizes and measuring times per step are given in Table 1. The diffractometer control and the data processing were handled with the software WinXPow 1.47 (STOE). The structure solution of the XRD data was done using the program EXPO [23], and for the refinement we used the program package WinPlotr/Fullprof [24]. Two of the Rietveld refinements plots, one for tetragonal $BiCaO_2NO_3$ and the other for orthorhombic $BiSrO_2NO_3$, are displayed in Fig. 1; the results of all four structure solutions are listed in Tables 1 and 2; selected distances and angles are given in Table 3. The unit cells of $BiPbO_2NO_3$ (isostructural with $BiCaO_2NO_3$) and $BiSrO_2NO_3$ (isostructural with $BiBaO_2NO_3$) are shown in Figs. 2a and b.

2.2. Infrared spectra

Infrared data were recorded on a FT-IR-Spectrometer (Spectrum 1000, Perkin Elmer) from pellets of $BiMO_2NO_3$ with KBr. The infrared spectra of all the investigated oxide nitrates show characteristic signals of nitrate ions (Table 4).

2.3. Thermal behavior

Thermogravimetric measurements (TG) and differential thermal analysis (DTA) were performed with a Netzsch Thermal Analyzer STA 409 under an oxygen/nitrogen flow (8% O_2). The $BiMO_2NO_3$ samples were heated up to 850°C in a corundum crucible using a heating rate of 2°C/min. The endothermic decomposition of $BiPbO_2NO_3$ occurs between 500°C and 570°C. At room temperature, a solid melt was left over in the sample carrier which could not be fully analyzed. The TG curve shows a mass loss of approximately 11.0%. The endothermic decomposition of $BiCaO_2NO_3$ occurs between 520°C and 570°C, yielding $Bi_2Ca_2O_5$ as identified by means of X-ray powder diffraction. The TG curve shows a mass loss of 15.8% (calculated: 15.74%).

The endothermic decomposition of $BiSrO_2NO_3$ occurs between 570°C and 650°C, yielding $Bi_2Sr_2O_5$ as identified by means of X-ray powder diffraction. The TG curve shows a mass loss of 14.0% (calculated: 13.82%).

The endothermic decomposition of $BiBaO_2NO_3$ occurs between 580°C and 640°C, yielding $BaBiO_3$ as identified by means of X-ray powder diffraction. The TG curve shows a mass loss of 11.6% (calculated: 11.45%).

3. Crystal structures and discussion

For M= Pb and Ca, both metal ions in the $BiMO_2NO_3$ structures occupy the same crystallographic position (4e: 0,0,z) supposing that Bi^{3+} and M^{2+} are statistically distributed over the same site (Figs. 2a

Table 1
Crystal data, experimental conditions for X-ray powder diffraction, data collection, structure refinement, and results for the oxide nitrates $BiMO_2NO_3$ (M= Pb, Ca, Sr, Ba)

Crystal data				
Empirical formula	$BiPbO_2NO_3$	$BiCaO_2NO_3$	$BiSrO_2NO_3$	$BiBaO_2NO_3$
Formula weight	510.185	343.060	390.600	440.307
Crystal system	tetragonal	tetragonal	orthorhombic	orthorhombic
Space group	*I*4/*mmm* (139)	*I*4/*mmm* (139)	*Cmmm* (65)	*Cmmm* (65)
Lattice parameters (pm)	$a = 397.199(4)$	$a = 396.337(5)$	$a = 1448.76(3)$	$a = 1536.50(8)$
	$c = 1482.57(2)$	$c = 1412.82(3)$	$b = 567.62(1)$	$b = 571.67(3)$
			$c = 582.40(1)$	$c = 597.55(3)$
Volume (10^6 pm^3)	233.901(5)	221.931(6)	478.93(3)	524.88(4)
Z	2	2	4	4
Density (calc.) (g cm^{-3})	7.243	5.133	5.417	5.573
Color	Yellow	White	White	Yellow
Data collection				
Temperature (K)	298	298	298	298
Wavelength (Cu$K\alpha_1$) (pm)	154.060	154.060	154.060	154.060
Scan range (°(2θ))	5–130	5–130	5–130	5–130
Step size (°(2θ))	0.5	0.5	0.5	0.5
Step time (s)	120	180	100	120
No. of single indexed lines	86	80	265	306
No. of refined parameters	23	23	30	30
Refinement				
Used program	Fullprof [24]	Fullprof [24]	Fullprof [24]	Fullprof [24]
R_p/R_{wp}	0.0989/0.1420	0.0795/0.1120	0.0707/0.0992	0.0803/0.1070
R_{Bragg}/R_F	0.0521/0.0443	0.0555/0.0558	0.0574/0.0392	0.0682/0.0477
χ^2	4.89	3.49	3.85	2.16

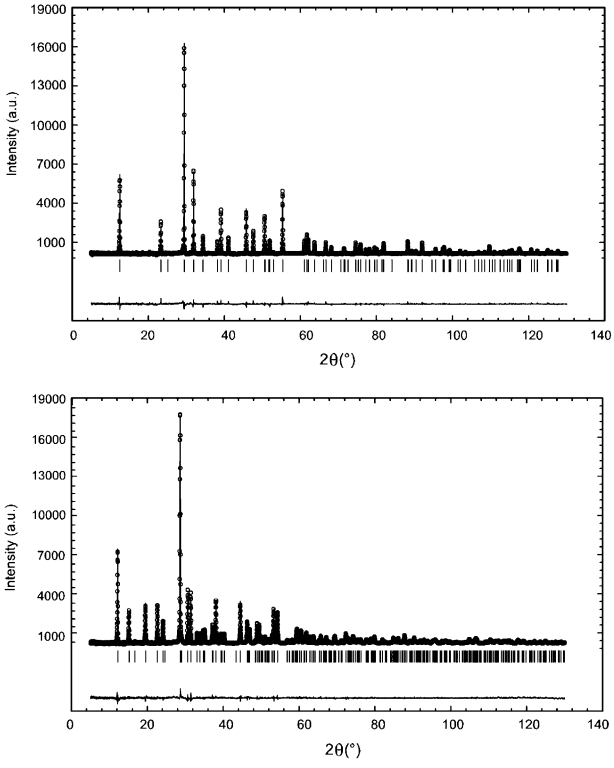

Fig. 1. Final Rietveld plots for $BiCaO_2NO_3$ (top) and $BiSrO_2NO_3$ (bottom) with measured pattern (solid line), calculated pattern (dotted line), calculated Bragg positions, and difference curve.

and 3a). The cation disorder may be caused by different reasons: the similar ionic radii of Bi^{3+} (103 pm) and Ca^{2+} (100 pm) promote the ideal tetragonal structure; for M= Pb, the cation disorder (that also occurs in the respective iodide) has been assumed to be due to the same electronic configuration of Bi^{3+} and Pb^{2+} ($6s^2$) [9]. Thus both $BiPbO_2NO_3$ and $BiCaO_2NO_3$ crystallize in the same space group (*I*4/*mmm*) as their respective oxide iodides (which differ from the oxide chlorides, as has been pointed out in the introduction). Together with the oxide ions O1, the metal atoms form $[BiMO_2]^+$ layers perpendicular to [001]. As F^- in the fluorite-type structure (CaF_2), the oxide ions occupy tetrahedral interstices of the metal ion arrangement. Four out of six of these $[OBi_2M_2]$ tetrahedra are shared with others to form plane layers just like in the lithargite structure of red PbO [26]. These layers are connected by orientally disordered nitrate $(NO_3)^-$ groups located in a tetragonal prismatic environment of eight metal ions. Structural models have been refined for the oxygen disorder of the nitrate groups in all four crystal structures at room temperature (selected distances and angles are given in Table 3). For M= Pb and Ca, a superposition of four different orientations of the nitrate group is given (Fig. 2a). For M= Sr and Ba, only two distinct orientations are obtained for both independent nitrate ions (Fig. 2b). Of course our disorder models cannot be

Table 2
Wyckoff positions, atomic coordinates, isotropic thermal displacement parameters, and site occupation factors for the oxide nitrates $BiMO_2NO_3$ (M= Pb, Ca, Sr, Ba)

Atom	Wyck	x/a	y/b	z/c	U_{eq}[a] (Å^2)	Occ.
$BiPbO_2NO_3$						
Bi	4*e*	0	0	0.16791(5)	0.0128(3)	0.5
Pb	4*e*	0	0	0.16791(5)	0.0128(3)	0.5
O1	4*d*	0.5	0	0.25	0.021(3)	1
N1	2*b*	0.5	0.5	0	0.09(1)	1
O11	4*e*	0.5	0.5	0.097(2)	0.021(3)	0.5
O12	16*n*	0.222(5)	0.5	0.040(1)	0.021(3)	0.25
$BiCaO_2NO_3$						
Bi	4*e*	0	0	0.1747(1)	0.0111(5)	0.5
Ca	4*e*	0	0	0.1747(1)	0.0111(5)	0.5
O1	4*d*	0.5	0	0.25	0.030(3)	1
N1	2*b*	0.5	0.5	0	0.10(1)	1
O11	4*e*	0.5	0.5	0.085(2)	0.030(3)	0.5
O12	16*n*	0.241(5)	0.5	0.058(2)	0.030(3)	0.125
$BiSrO_2NO_3$						
Bi	4*h*	0.18103(8)	0.5	0.5	0.0131(5)	1
Sr	4*g*	0.3434(1)	0.5	0	0.0083(8)	1
O1	8*m*	0.25	0.75	0.727(2)	0.016(2)	1
N1	2*d*	0	0	0.5	0.06(1)	1
O11	4*k*	0	0	0.256(5)	0.016(2)	0.5
O12	8*o*	0.079(2)	0	0.435(4)	0.016(2)	0.5
N2	2*b*	0	0.5	0	0.06(1)	1
O21	4*i*	0	0.248(5)	0	0.016(2)	0.5
O22	8*p*	0.073(1)	0.430(4)	0	0.016(2)	0.5
$BiBaO_2NO_3$						
Bi	4*h*	0.1846(1)	0.5	0.5	0.0114(8)	1
Ba	4*g*	0.3456(1)	0.5	0	0.006(1)	1
O1	8*m*	0.25	0.75	0.742(2)	0.055(5)	1
N1	2*d*	0	0	0.5	0.15(1)	1
O11	4*k*	0	0	0.291(7)	0.055(5)	0.5
O12	8*o*	0.070(2)	0	0.412(6)	0.055(5)	0.5
N2	2*b*	0	0.5	0	0.15(1)	1
O21	4*i*	0	0.285(9)	0	0.055(5)	0.5
O22	8*p*	0.072(2)	0.398(5)	0	0.055(5)	0.5

[a] $U_{eq} = 1/3(U_{11} + U_{22} + U_{33})$.

Table 3
Selected interatomic distances (pm) and angles (°) for the oxide nitrates $BiMO_2NO_3$ (M= Pb, Ca, Sr, Ba)

Compound	$BiPbO_2NO_3$	$BiCaO_2NO_3$	$BiSrO_2NO_3$	$BiBaO_2NO_3$
Bi–O1	232.9(1)	224.9(1)	218.2(7)	226.8(8)
Bi–N1	375.3(1)	373.4(1)	386.4(1)	402.7(1)
Bi–N2			391.9(1)	412.0(1)
M–O1	232.9(1)	224.9(1)	252.4(7)	256.5(7)
M–N1	375.3(1)	373.4(1)	369.1(1)	381.5(1)
M–N2			363.3(1)	371.5(1)
N1–O11	144(3)	120(3)	142(3)	125(4)
N1–O12	125(2)	131(2)	122(3)	120(3)
N2–O21			143(3)	123(5)
N2–O22			113(2)	125(3)
O11–N1–O12	118.2(7)	129(1)	108(1)	116(2)
O12–N1–O12	124(1)	103(1)	143(2)	128(2)
O21–N2–O22			111(1)	118(1)
O22–N2–O22			139(1)	124(2)

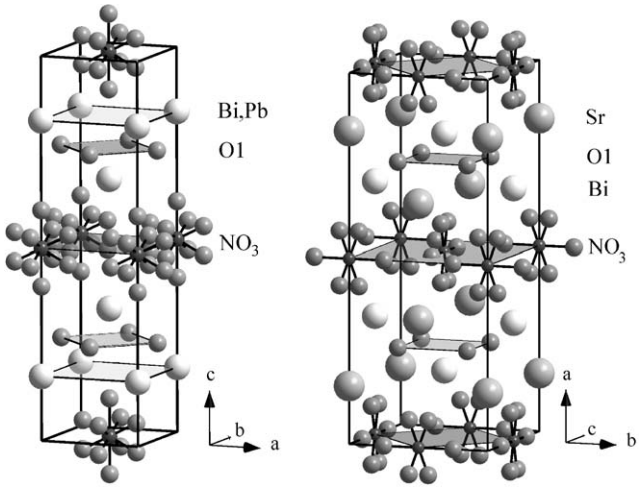

Fig. 2. Unit cells of: (a) $BiPbO_2NO_3$ and (b) $BiSrO_2NO_3$.

considered as fully reliable because it is difficult to determine the position of the light atoms (N and O) in contrast to the heavy atoms using powder XRD. We assume that our results are reasonable as we achieved stable refinements of the parameters of the light atoms. The nitrogen atoms show very large temperature factors; one reason could be that the N positions have to be split, leading to more symmetrical nitrate ions. However, calculations that took such split N positions into account did not lead to stable refinements.

The noticeable increase of the lattice constant c from 1352.0(2) pm in $BiPbO_2I$ [3] to 1482.57(2) pm in $BiPbO_2NO_3$ and from 1321.44(1) pm in $BiCaO_2I$ [9] to 1412.82(3) pm in $BiCaO_2NO_3$ and the decrease of the lattice constant a may be explained by the specific orientation of the nitrate groups (Fig. 2a). The O11 atom points along the $\pm$[001] direction, and thus provides a larger separation between the adjacent $[BiMO_2]^+$ layers in $BiMO_2NO_3$ compared to $BiMO_2I$. The larger lattice constant c of $BiPbO_2NO_3$ compared with $BiCaO_2NO_3$ results mainly from the larger ionic radius of Pb^{2+} (119 pm) versus Ca^{2+} (100 pm): The (Bi,Pb)–O1 distances are 232.9(1) pm, while the (Bi,Ca)–O1 separations only amount to 224.9(1) pm.

In the $BiMO_2NO_3$ compounds with M= Sr and Ba, the atoms are displaced from the tetragonal formations, thus lowering the crystal symmetry and generating an orthorhombic superstructure (Figs. 2b and 3b), as also observed for the pair lithargite [26] and massicot (yellow PbO, orthorhombic) [27]. This cation ordering of Bi^{3+} and M^{2+}, which occurs due to noticeably larger ionic radii of M^{2+} (Bi^{3+}: 103 pm; Sr^{2+}: 118 pm; Ba^{2+}: 135 pm), has also been reported for their respective oxide halides [9,14,15] and compounds with lead or

Table 4
Fundamental wavenumbers (in cm^{-1}) of $[NO_3]^-$ in $BiONO_3 \cdot H_2O$, $BiPbO_2NO_3$, $BiCaO_2NO_3$, $BiSrO_2NO_3$, and $BiBaO_2NO_3$ with their relative intensities and assignments; v = very, s = strong; m = medium; w = weak

$BiONO_3 \cdot H_2O$ [25]		$BiPbO_2NO_3$		$BiCaO_2NO_3$		$BiSrO_2NO_3$		$BiBaO_2NO_3$		Assignment
716	vw	723	vw	743	vw	735	vw	729	vw	ν_4 (E)
825	s	812	m	820	m	816	m	822	s	ν_2 (A_2)
1051	w	1042	w	1044	w	1060	w	1052	w	ν_1 (A_1)
—		1366	vs	1346	vs	1352	vs	1361	vs	
1385	vs	1384	vs	1385	vs	1364	vs	1384	vs	ν_3 (E)
1433	s	—		1429	s	1430	s	1435	s	

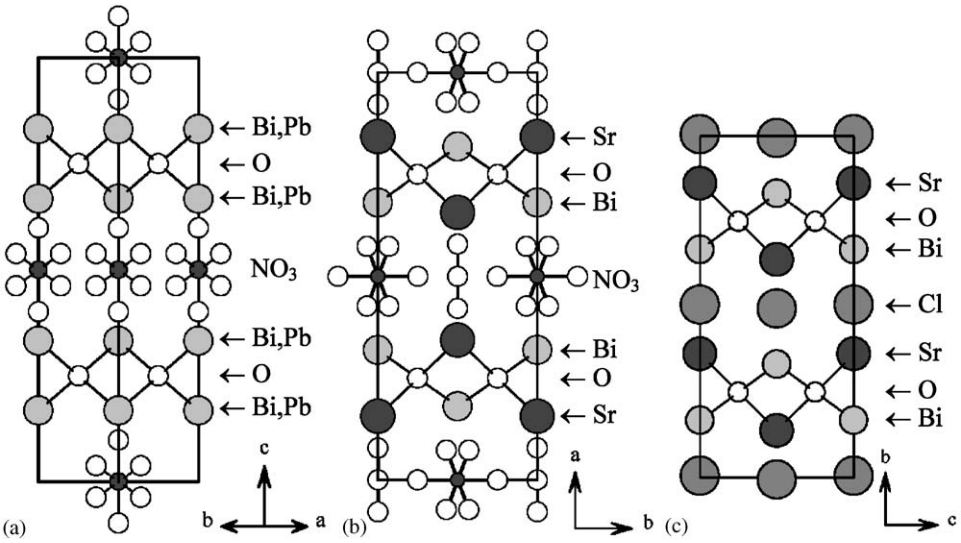

Fig. 3. Crystal structures of three variants of the Sillén X_1 type. From left to right: (a) $BiPbO_2NO_3$ (tetragonal), (b) $BiSrO_2NO_3$ (orthorhombic), (c) $BiSrO_2Cl$ (orthorhombic). Note the different cation ordering schemes for (b) and (c).

antimony [16–20], which crystallize in the orthorhombic space group *Cmcm* (Fig. 3c). However, the orthorhombic superstructure of the oxide nitrates is distinctly different: the cation ordering of Bi^{3+} and M^{2+} forms upon another pattern, bringing about a new layer sequence (see Fig. 3b) and symmetry with the space group *Cmmm*.

Comparable with the tetragonal $BiMO_2NO_3$ compounds, the long lattice constants in $BiMO_2NO_3$, with M = Sr, Ba, are significantly larger than in their respective oxide iodides, while the small constants are shorter, due to the particular orientations of nitrate groups (Fig. 2b).

In the course of our investigations, we discovered that it is possible to exchange or mix the M^{2+} cations with each other in the $BiMO_2NO_3$ compounds. Calibration curves for the solid solutions $BiPb_xCa_{1-x}O_2NO_3$ and $BiSr_xCa_{1-x}O_2NO_3$ have been presented [28,29]. This ionic compatibility and some other properties like their layer-type structure and stability under NO_x atmosphere make the $BiMO_2NO_3$ compounds interesting precursors for oxide materials, e.g., the HTSC compounds $(Bi,Pb)_2Sr_2Ca_{n-1}Cu_nO_x$ [30]. In this context, $BiSrO_2NO_3$ was used as an intermediate phase for a new synthesis route of $Bi_2Sr_2CuO_{6+\delta}$ ("Bi-2201") under NO_x atmosphere [31]. The compounds with mixed M^{2+} cations (M = Pb, Sr, Ca) were used as precursors in the thoroughly investigated new synthesis routes for Bi(Pb)–2212 [28] and the 110 K superconductor (Bi,Pb)–2223 [29].

References

[1] L.G. Sillén, Z. Anorg. Allg. Chem. 242 (1939) 41.
[2] L.G. Sillén, Naturwissenschaften 30 (1942) 318k.
[3] J. Ketterer, V. Krämer, Mater. Res. Bull. 20 (1985) 1031.
[4] L.G. Sillén, Svensk. Kem. Tidskr. 53 (1941) 39.
[5] L.G. Sillén, Z. Anorg. Allg. Chem. 246 (1941) 115.
[6] J.F. Ackerman, Mater. Res. Bull. 17 (1982) 883.
[7] W. Nieuwenkamp, J.M. Bijvoet, Z. Kristallogr. 81 (1932) 469.
[8] Z. Ban, M. Sikirica, Acta Crystallogr. 18 (1965) 594.
[9] D.O. Charkin, P.S. Berdonosov, V.A. Dolgikh, P. Lightfoot, J. Solid State Chem. 175 (2003) 316.
[10] A. Lagercrantz, L.G. Sillén, Ark. Kemi Mineral. Geol. 25 (1948) 1.
[11] H. Boller, Monatsh. Chem. 104 (1973) 916.
[12] P.M. Raccah, J.M. Longo, H.A. Eick, Inorg. Chem. 6 (1967) 1471.

[13] Y. Hashimoto, M. Takahashi, S. Kikkawa, F. Kanamaru, J. Solid State Chem. 114 (1995) 592.
[14] S.M. Fray, C.J. Milne, P. Lightfoot, J. Solid State Chem. 128 (1997) 115.
[15] M.A. Kennard, J. Darriet, J. Grannec, A. Tressaud, J. Solid State Chem. 117 (1995) 201.
[16] F. Thuillier-Chevin, P. Maraine, G. Perez, Rev. Chim. Miner. 17 (1980) 102.
[17] L.G. Sillén, L. Melander, Z. Kristallogr. 103 (1941) 420.
[18] A. Deschanvres, J. Gallay, J.-M. Hunout, M.-Th. Thiault, C. Victor, C. R. Acad. Sci. Paris 270 (1970) 696.
[19] Y. Porter, P.S. Halasyamani, Z. Naturforsch. 57b (2002) 360.
[20] M. Gillberg, Ark. Kemi Mineral. Geol. 2 (1961) 565.
[21] H. Kodama, in: A. Dyer, M.J. Hudson, P.A. Williams (Eds.), Progress in Ion Exchange, The Royal Society of Chemistry 196, 1997, pp. 39.
[22] H. Kodama, Japanese Patent 2000086243, Science and Technology Agency, National Institute for Research in Inorganic Materials, Japan, 1998.
[23] A. Altomare, M.C. Burla, M. Camalli, G. Cascarano, C. Giacovazzo, A. Guagliardi, A.G.G. Moliterni, R. Rizzi, EXPO: a program for full powder pattern decomposition and crystal structure solution, J. Appl. Crystallogr. 32 (1998) 339.
[24] T. Roisnel, J. Rodríguez-Carvajal, WinPLOTR: a Windows tool for powder diffraction patterns analysis, Materials Science Forum, in: R. Delhez, E.J. Mittemeijer (Eds.), Proceedings of the Seventh European Powder Diffraction Conference (EPDIC 7), Barcelona, 2000, pp. 118.
[25] R.A. Nyquist, R.O. Kagel, C.L. Putzig, M.A. Leugers, Handbook of Infrared and Raman Spectra of Inorganic Compounds and Organic Salts, Vol. 3. Infrared Spectra, Academic Press, San Diego, 1996, p. 77.
[26] R.G. Dickinson, J.B. Friauf, H. Boller, J. Am. Chem. Soc. 46 (1924) 2457.
[27] R.J. Hill, Acta Crystallogr. C 41 (1985) 1281.
[28] K. Gibson, P. Ziegler, H.-J. Meyer, Supercond. Sci. Technol. 17 (2004) 786.
[29] K. Gibson, P. Ziegler, H.-J. Meyer, Physica C 403 (2004) 1.
[30] P. Ziegler, K. Gibson, H.-J. Meyer, German Patent Specification PCT/EP03/08861, DE 10261549.7 Patentamt München, 2002.
[31] K. Gibson, P. Ziegler, H.-J. Meyer, Physica C 397 (2003) 112.